Thermodynamic Stability of Carbonic Anhydrase: Measurements of Binding Affinity and Stoichiometry Using ThermoFluor

Daumantas Matulis,‡ James K. Kranz, F. Raymond Salemme, and Matthew J. Todd*

Johnson & Johnson Pharmaceutical Research & Development, LLC, Eagleview Corporate Center, 665 Stockton Drive, Suite 104, Exton, Pennsylvania 19341

Received August 30, 2004; Revised Manuscript Received December 3, 2004

ABSTRACT: ThermoFluor (a miniaturized high-throughput protein stability assay) was used to analyze the linkage between protein thermal stability and ligand binding. Equilibrium binding ligands increase protein thermal stability by an amount proportional to the concentration and affinity of the ligand. Binding constants (K_b) were measured by examining the systematic effect of ligand concentration on protein stability. The precise ligand effects depend on the thermodynamics of protein stability: in particular, the unfolding enthalpy. An extension of current theoretical treatments was developed for tight binding inhibitors, where ligand effect on T_m can also reveal binding stoichiometry. A thermodynamic analysis of carbonic anhydrase by differential scanning calorimetry (DSC) enabled a dissection of the Gibbs free energy of stability into enthalpic and entropic components. Under certain conditions, thermal stability increased by over 30 °C; the heat capacity of protein unfolding was estimated from the dependence of calorimetric enthalpy on T_m. The binding affinity of six sulfonamide inhibitors to two isozymes (human type 1 and bovine type 2) was analyzed by both ThermoFluor and isothermal titration calorimetry (ITC), resulting in a good correlation in the rank ordering of ligand affinity. This combined investigation by ThermoFluor, ITC, and DSC provides a detailed picture of the linkage between ligand binding and protein stability. The systematic effect of ligands on stability is shown to be a general tool to measure affinity.

Numerous techniques have been introduced for measuring ligand binding affinity to macromolecules of pharmacological interest. Many of these tools lack generality and must be optimized for each target, requiring significant development time. Some techniques are broadly applicable, such as the perturbing effects of ligand binding on protein stability and the determination of binding affinity from these perturbations. Ligands that interact preferentially with native proteins will increase protein stability; ligands that interact preferentially with the non-native forms of the proteins will decrease protein stability.

Methods to measure binding via perturbations in protein thermodynamic stability toward chemical or thermal insults have been developed (*1*). To assess protein thermal stability, the experimental temperature is increased and some parameter of protein structure is measured. A temperature is reached above which a protein's native structure is less thermodynamically favorable, and the protein unfolds. T_m is defined as a midpoint in a thermal ramp and represents a temperature where the free energy of the native and non-native forms are equivalent.

Ligand-induced perturbations in thermal stability are observed experimentally as a change in the protein T_m. The size of T_m change is proportional to both the ligand concentration and the binding affinity. This phenomenon is well understood and has been used previously to determine protein−ligand binding constants (*2*). Protein melting temperatures can be determined by numerous methods, including differential scanning calorimetry (*3*, *4*) and optical methods (circular dichroism (*5*), fluorescence or absorbance spectroscopy). Fluorometrically, thermal stability can be measured by using changes in intrinsic tryptophan fluorescence (*6*) or by monitoring changes in an environmentally sensitive fluorescent probe such as ANS[1] (*7*). These techniques have low throughput, are time consuming, and require significant amounts of protein and, thus, are not generally utilized when testing the large numbers of compounds generated during drug development.

The value of a universal binding assay to the pharmaceutical industry could be significant. Many companies have accumulated large libraries of organic molecules that are tested in search of activity toward molecular targets. Using stability perturbations to screen compound libraries or to confirm binding is an attractive tool for numerous reasons: (1) *all* compounds that bind at *any* site are detected, including active site(s), allosteric/regulatory sites, and sites of protein−protein interactions; (2) there is no theoretical maximum to

* To whom correspondence should be addressed. E-mail: Mtodd3@prdus.jnj.com. Tel: 610-458-6062. Fax: 610-458-8249.

‡ Current address: Institute of Biotechnology, Graiciuno 8, Vilnius, Lithuania.

[1] Abbreviations: ANS, 1-anilino-8-naphthalenesulfonate; ACTAZ, acetazolamide; *h*-CAI, carbonic anhydrase, isozyme I, from human erythrocytes; *b*-CAII, carbonic anhydrase, isozyme II, from bovine erythrocytes; CCD, charge coupled device; DCPHA, dichlorophenamide; DMSO, dimethyl sulfoxide (methyl sulfoxide); DSC, differential scanning calorimetry; ITC, isothermal titration calorimetry; MES, 2-morpholinoethanesulfonic acid; METHZ, methazolamide; PAMBS, *p*-aminomethylbenzenesulfonamide; PIPES, piperazine-1,4-bis(2-ethanesulfonic acid); SULFA, sulfanilamide; TFMSA, trifluoromethanesulfonamide.

10.1021/bi048135v CCC: $30.25
Published on Web 03/09/2005

the affinity that can be measured (*8*); (3) these assays are not subject to the same interferences as optical assays. Additionally, binding assays are complimentary to enzymatic or cell-based assays, as an orthogonal determination of activity. Compounds that show activity across several different types of assays have a higher probability of becoming sustainable leads and are thus more desirable to pursue.

ThermoFluor offers several advantages over classical thermal denaturation measurements: the generality of using a common Fluor (such as ANS), a large reduction in volume, and the ability to parallelize measurements in high-density format. ThermoFluor measures the change in fluorescence of an environmentally sensitive dye on protein unfolding (*9*). These dyes are quenched in aqueous environments but have a large increase in quantum yield when bound to the hydrophobic interior of a protein. An intrinsic fluorescence probe (e.g. Tyr or Trp) could be exploited; however, the use of an external probe offers several advantages: (1) an external probe is likely to have similar behavior for many proteins, (2) the fluorescence of an external probe is less likely to be affected by compound binding to native protein, (3) the higher excitation and emission wavelengths plus the large Stokes shift reduces interference from fluorescent compounds, and (4) the optimal wavelengths of an external probe are less likely to be protein dependent. Assays are performed in volumes of less than 4 μL in 384-well PCR thermocycler plates and imaged using CCD detection, which enables an array of conditions or compounds to be assayed simultaneously. The T_m value is determined with high precision (s.d. $<$ 0.2 °C, $n = 384$); thus, a multiplicity of reaction conditions, potential inhibitors, or inhibitor concentrations can be tested in parallel.

Carbonic anhydrase (EC 4.2.1.1) is a clinically relevant and biochemically well-characterized protein (*10*). It catalyzes hydration of carbon dioxide to carbonic acid (*11, 12*) and is involved in vital physiological processes such as pH and CO_2 homeostasis, transport of bicarbonate and CO_2, biosynthetic reactions, bone resorption, calcification, tumorigenicity, and other physiological or pathological processes. Therefore, this enzyme is an important target for inhibitors with clinical applications, primarily for use as antiglaucoma agents but also for the therapy of various pathologies such as epilepsy and Parkinson's disease.

Affinity constants for sulfonamide inhibitors binding to carbonic anhydrase were determined by measuring the T_m values at various ligand concentrations to generate a concentration response curve in ThermoFluor. Models relating the ligand-dependent increase in protein thermal stability to association constants require an accurate knowledge of the thermodynamics of protein stability. Thus, carbonic anhydrase stability was studied by differential scanning calorimetry (DSC), giving a complete thermodynamic description of the Gibbs free energy, calorimetric enthalpy, and heat capacity of unfolding ($\Delta_U G_{(T)}$, $\Delta_U H_{(T)}$, and $\Delta_U C_p$, respectively).

Models relating ligand-dependent increases in protein thermal stability also rely on accurate knowledge of the ligand concentration (*2, 13*). For tight binding ligands, the free ligand concentration may be significantly less than the total ligand concentration, due to that which is bound. We present a mathematical model linking the effect of ligand and protein concentration on thermal stability that considers depletion of total ligand by that which is bound. This model correctly predicts concentration-dependent changes in T_m for both tight and weak binding ligands. These affinity constants are then compared to those obtained by isothermal titration calorimetry (ITC).

MATERIALS AND METHODS

Materials. Crystalline protein (*h*-CAI, Sigma, cat. # C4396; *b*-CAII, Sigma, cat. # C2522) was dissolved in buffer and passed through a desalting column (Sephadex G-25M, PD-10, Pharmacia) before use. Concentrations were determined by weight and by spectrophotometry (discrepancy between methods did not exceed 15%) using $\epsilon_{280nm} = 49{,}000$ and 52,000 $M^{-1}cm^{-1}$ for *h*-CAI and *b*-CAII, respectively. Inhibitors (Figure 1) were from Lancaster Synthesis (TFMSA) or Sigma Chemical Co.

ThermoFluor. ThermoFluor experiments were carried out using instruments available from Johnson & Johnson Pharmaceutical Research & Development, LLC, Exton, PA[2]. Protein−ligand solutions (1−4 μL) were dispensed into black 384-well polypropylene PCR microplates (Abgene) and overlayed with silicone oil ($\leq$1 μL, Fluka, type DC 200, cat. #85411) to prevent evaporation. Protein solutions contained 0.01−1 mg/mL carbonic anhydrase, 25−50 mM buffer, 50−100 mM NaCl, 0−2% DMSO, 50−100 μM ANS, 0−50 μM $ZnCl_2$, 0−1.0 mM EDTA, and 0−2.0 mM inhibitor, as described in the figure legends. Bar-coded thermocycler plates were robotically loaded onto a thermostatically controlled PCR-type thermal block and then heated at a rate of 1 °C/min for all experiments. Fluorescence was measured by continuous illumination with UV light (Hamamatsu LC6) supplied via fiber optic and filtered through a bandpass filter (380−400 nm; >6 OD cutoff). Fluorescence emission of the entire 384-well plate was detected by measuring light intensity using a CCD camera (Sensys, Roper Scientific) filtered to detect 500 $\pm$ 25 nm, resulting in simultaneous and independent readings of all 384 wells. One or more images were collected at each temperature, and the sum of the pixel intensity in a given area of the Thermocycler plate was recorded vs temperature. The typical imaging time was 2−30 s. If multiple images were collected at a given temperature, the intensity per well of these images was averaged. Reference wells contained protein without inhibitor.

DSC Experiments. Differential scanning calorimetry experiments were carried out using a VP-DSC calorimeter (Microcal, Inc., North Hampton, MA). *b*-CA II was 0.12−0.20 mg/mL (0.4 mL cell) in 25 mM sodium acetate or PIPES (pH as indicated in the text), 100 mM NaCl, $\pm$0.5 mM EDTA, $\pm$50 μM ANS, and $\pm$100 μM ACTAZ. Calorimetric enthalpy was determined by integrating the area under the peak after adjusting the pre- and post-transition baselines. van't Hoff enthalpy of unfolding was determined by fitting thermograms to a two-state reversible unfolding model.

[3] The ThermoFluor assay was developed by 3-Dimensional Pharmaceuticals, Inc., which has been merged into Johnson & Johnson Pharmaceutical Research & Development, LLC. "ThermoFluor" is a trademark registered in the United States and certain other countries and is protected under US patents US6020141, US6036920, US6214293, US6232085, US6268158, US6268218, US6291191, US6291192, and US6303322 (*9*).

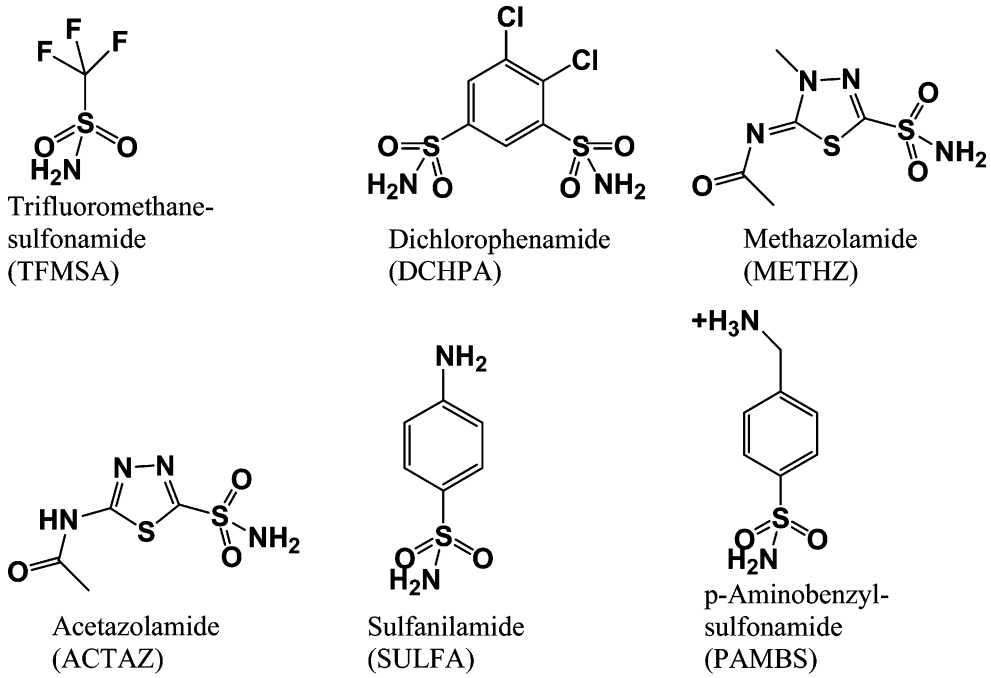

FIGURE 1: Chemical structures and abbreviations of the six carbonic anhydrase inhibitors used in this study.

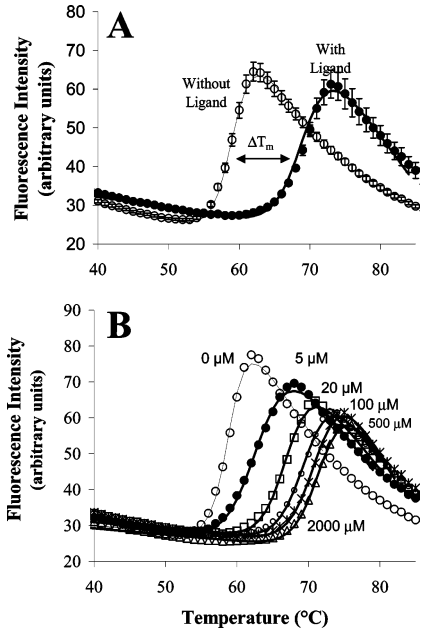

FIGURE 2: Inhibitor stabilization of *h*-CA I as measured by ThermoFluor. (A) Reaction mixtures contained 4 μL of 8.3 μM *h*-CAI, in 25 mM MES, pH 6.1, 50 mM NaCl, 50 μM ANS, 2% DMSO plus 0 mM (○) or 100 μM (●) TFMSA. Reaction mixtures were heated at 1 °C/min and imaged every 0.5 °C. Integrated intensity from quadruplicate reactions (averages given by symbols, deviations given by bars) was fit to eq 6 as described in Materials and Methods (lines) to obtain the midpoint, or T_m. Nonlinearity in the post-transition baseline is related to the temperature dependence of ANS affinity to non-native protein. (B) *h*-CA I unfolding at various TFMSA concentrations. Reaction mixtures contained 4 μL of 11 μM *h*-CAI, in 25 mM MES, pH 6.1, 50 mM NaCl, 50 μM ANS, 2% DMSO plus 0 μM (○), 5 μM (●), 20 μM (□), 100 μM (○), 500 μM (*), or 2000 μM (△) as described above. Data fit to eq 6 gave a midpoint (T_m) of 59.0, 63.3, 67.4, 70.0, 71.6, and 72.2 °C, respectively.

Protein Unfolding Curves. Fluorescence intensity in protein denaturation curves (Figure 2) can be described by the equations

$$y(T) = y_F + \frac{y_U - y_F}{1 + e^{\Delta_U G_{(T)}/RT}} = y_U + \frac{y_F - y_U}{1 + e^{-\Delta_U G_{(T)}/RT}} \quad (1)$$

where y_F and y_U are the fluorescence intensity of ANS in the presence of native and non-native protein, respectively, and the exponential represents the probability of a protein with free energy $\Delta_U G_{(T)}$ being unfolded. Both initial and final fluorescence intensities change with temperature and can be approximated as linear dependencies:

$$y_{F(T)} = y_{F,T_m} + m_F(T - T_m) \quad (2)$$

$$y_{U(T)} = y_{U,T_m} + m_U(T - T_m) \quad (3)$$

where y_{F,T_m} and y_{U,T_m} are fluorescence intensities of ANS in the presence of native and non-native protein at the melting temperature T_m, and m_F and m_U are the linear temperature dependences of ANS fluorescence intensity plus native and non-native protein, respectively.

The Gibbs free energy as a function of temperature ($\Delta_U G_{(T)}$) can be expressed in terms of the enthalpy ($\Delta_U H_{T_r}$), entropy ($\Delta_U S_{T_r}$), and heat capacity ($\Delta_U C_p$) of protein unfolding at a reference temperature T_r, which was chosen to be T_m in the absence of ligand:

$$\Delta_U G_{(T)} = \Delta_U H_{(T)} - T\Delta_U S_{(T)} = \Delta_U H_{T_r} + \Delta_U C_p(T - T_r) - T\left(\Delta_U S_{T_r} + \Delta_U C_p \ln\left(\frac{T}{T_r}\right)\right) \quad (4)$$

The heat capacity was assumed to be temperature-independent over a small range in temperature. For a two-state reversible unfolding transition, $\Delta_U G_{T_r} = 0$ at the T_m value; thus, the enthalpy and entropy of unfolding are related as

$$\Delta_U H_{T_r} = T\Delta_U S_{T_r} \quad (5)$$

Because this relationship is only true at the melting temperature in the absence of ligand (T_r), it was not used to simplify

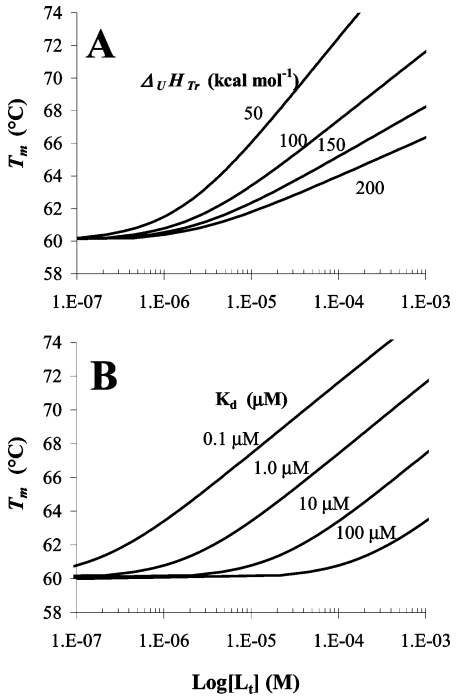

FIGURE 3: Ligand effect on protein T_m is protein specific and is proportional to the $\Delta_U H_{T_r}$. A) The following parameters were used to simulate concentration response curves for different proteins (eq 14), assuming constant ligand binding affinity. Ligand binding parameters: $K_{b,T_0=37°C} = 10^6$ M^{-1} ($K_d = 1$ μM), $\Delta_b H_{T_0=37°C} = -5.0$ kcal mol^{-1}, $\Delta_b C_p = -0.2$ kcal mol^{-1} K^{-1}. Protein stability parameters: $T_r = 60$ °C, $\Delta_U C_p = 1.5$ kcal mol^{-1} K^{-1}, and the indicated $\Delta_U H_{T_r}$. (B) For a given protein, $\Delta_U H_{T_r}$ will be constant, and the effect of ligand on protein T_m will be proportional to both concentration and affinity (eq 8). The following parameters were used in eq 14 to simulate curves. Protein stability parameters: $\Delta_U H_{T_r} = 100$ kcal mol^{-1}, $\Delta_U C_p = 1.5$ kcal mol^{-1} K^{-1}, $T_r = 60$ °C. Ligand binding parameters: $\Delta_b H_{T_0=37°C} = -5.0$ kcal mol^{-1}, $\Delta_b C_p = -0.2$ kcal mol^{-1} K^{-1}. K_d (in μM) is indicated in the figure.

equations for ligand effect on protein stability as a function of temperature.

After eqs 1−4 are combined, the final equation used to fit protein melting curves shown in Figure 2 is

$$y_{(T)} = y_{F,T_m} + m_F(T - T_m) + \frac{y_{U,T_m} - y_{F,T_m} + (m_U - m_F)(T - T_m)}{1 + e^{(\Delta_U H_{Tr} + \Delta_U C_p(T - T_r) - T(\Delta_U S_{Tr} + \Delta_U C_p \ln(T/T_r)))/RT}} \quad (6)$$

The six parameters y_{F,T_m}, m_F, y_{U,T_m}, m_U, $\Delta_U H_{T_r}$, and T_m were fit using the Levenberg−Marquardt algorithm for minimizing the sum of the squares of the residuals. $\Delta_U C_p$ was kept constant, because it is poorly determined by this method. Reliable estimates for $\Delta_U C_p$ can be obtained from protein sequence or structural data if calorimetric characterization is not available (*14*, *15*). The standard deviation of T_m using ThermoFluor (averaged over 384 wells) is less than 0.2 °C.

Model: Protein T_m vs Ligand Concentration. When a ligand binds to the native protein, it shifts the equilibrium between unfolded and native species toward the native form:

$$U + L_f \underset{\text{folding}}{\overset{K_U}{\rightleftharpoons}} N + L_f \underset{\text{ligand binding}}{\overset{K_B}{\rightleftharpoons}} NL_b \quad (7)$$

where U = non-native protein, N = native protein, L_f = free ligand, and NL_b = complex between native protein and bound ligand. The observed stability of the protein is the sum of the protein stability in the absence of ligand ($\Delta_U G_{(T)}$) and an amount proportional to the affinity and concentration of the ligand:

$$\Delta G_{(T)} = \Delta_U G_{(T)} + \Delta_B G_{(T)} = \Delta_U G_{(T)} + RT \ln(1 + K_b[L_f]) \quad (8)$$

where $\Delta_B G_{(T)}$ is the additional stabilization free energy due to ligand binding. Note at the T_m value in the presence of ligand, $\Delta G_{(T)} = 0$; thus, $\Delta_U G_{(T)} = -RT \ln(1 + K_b[L_f])$.

The equilibrium constants for protein stability and ligand binding in eq 7 are related to the free energy of unfolding and binding by the equations

$$K_U = \frac{[U]}{[N]} = e^{-\Delta_U G_{(T)}/RT} = e^{-(\Delta_U H_{(T)} - T\Delta_U S_{(T)})/RT} = e^{-(\Delta_U H_{Tr} + \Delta_U C_p(T - T_r) - T(\Delta_U S_{Tr} + \Delta_U C_p \ln(T/T_r)))/RT} \quad (9)$$

$$K_b = \frac{[NL_b]}{[N][L_f]} = e^{-\Delta_b G_{(T)}/RT} = e^{-(\Delta_b H_T - T\Delta_b S_T)/RT} = e^{-(\Delta_b H_{T0} + \Delta_b C_p(T - T_0) - T(\Delta_b S_{T0} + \Delta_b C_p \ln(T/T_0)))/RT} \quad (10)$$

where $\Delta_U G_{(T)}$, $\Delta_U H_{(T)}$, $\Delta_U S_{(T)}$, and $\Delta_U C_p$ are temperature-dependent functions of the Gibbs free energy, enthalpy, entropy, and heat capacity of protein stability and $\Delta_b G_{(T)}$, $\Delta_b H_{(T)}$, $\Delta_b S_{(T)}$, and $\Delta_b C_p$ are temperature-dependent functions of the Gibbs free energy, enthalpy, entropy, and heat capacity of ligand binding. Equations for the conservation of mass of protein (P_t) and ligand (L_t)

$$P_t = [N] + [U] + [NL_b] \quad (11)$$

$$L_t = [L_f] + [NL_b] \quad (12)$$

can be combined with eq 8 and rearranged to give an expression for total concentration of ligand needed to stabilize a protein:

$$L_t = (1 - K_U)\left(\frac{P_t}{2} + \frac{1}{K_U K_b}\right) \quad (13)$$

Substituting eq 13 with eq 9 and eq 10 gives an expression of the total ligand concentration needed to raise the protein T_m to a given value:

$$L_t = (1 - e^{-(\Delta_U H_{Tr} + \Delta_U C_p(T - T_r) - T(\Delta_U S_{Tr} + \Delta_U C_p \ln(T/T_r)))/RT}) \times \left(\frac{P_t}{2} + 1/e^{-(\Delta_U H_{Tr} + \Delta_U C_p(T - T_r) - T(\Delta_U S_{Tr} + \Delta_U C_p \ln(T/T_r)))/RT} e^{-(\Delta_b H_{T0} + \Delta_b C_p(T - T_0) - T(\Delta_b S_{T0} + \Delta_b C_p \ln(T/T_0)))/RT}\right) \quad (14)$$

For weakly binding ligands, $P_t < K_d = K_b^{-1}$, and eq 14 simplifies to

$$L_t = \frac{1 - K_U}{K_U K_b} = (1 - e^{-(\Delta_U H_{Tr} + \Delta_U C_p(T - T_r) - T(\Delta_U S_{Tr} + \Delta_U C_p \ln(T/T_r)))/RT}) \times (1/e^{-(\Delta_U H_{Tr} + \Delta_U C_p(T - T_r) - T(\Delta_U S_{Tr} + \Delta_U C_p \ln(T/T_r)))/RT} e^{-(\Delta_b H_{T0} + \Delta_b C_p(T - T_0) - T(\Delta_b S_{T0} + \Delta_b C_p \ln(T/T_0)))/RT}) \quad (15)$$

as previously derived by Brandts and Lin (*2*) and Shrake and Ross (*13*). By including terms for the total protein, eq 14 can be used for tight-binding ligands at concentrations equivalent to the site concentration. Equations 14 and 15 are transcendental and, thus, cannot be solved explicitly for T_m as a function of L_t. Instead, curves were simulated by calculating the concentration of total added ligand (L_t) necessary to give an experimentally observed T_m.

RESULTS

ThermoFluor Protein Melts. The thermal stability of carbonic anhydrase, monitored using ANS fluorescence, is shown in Figure 2; ANS is highly quenched in an aqueous environment. As a protein unfolds, hydrophobic surfaces that are buried in the native protein became exposed to solvent; as ANS binds to these hydrophobic sites, the fluorescence intensity increases (*17*). Fluorescence intensity data from Figure 2 were fit to eq 6, giving six parameters: two parameters describe the initial linear baseline, two parameters describe the final linear baseline, and two parameters ($\Delta_U H_{T_m}$, T_m) describe the change in fluorescence as the protein unfolds. For much of this work, the only parameter considered was T_m, or the midpoint of the fluorescence transition. In experiments where multiple replicates of the same reaction conditions were examined simultaneously, deviations in T_m were small (±0.2 °C, error bars in Figure 2A).

Figure 2A shows a second reaction, run simultaneously, examining the effect of a known inhibitor on CAII thermal stability. The calculated T_m was higher than that in the absence of inhibitor, demonstrating how equilibrium binding ligands at concentrations higher than their K_d values increase protein stability. Methods to estimate binding affinity from changes in protein thermal stability using a single concentration of ligand have been published previously (*3*−*10*). A more accurate measure of the binding constant could be obtained by examining stability as a function of ligand concentration. As shown in Figure 2B, when a series of thermal melts were collected with varying concentrations of inhibitor, the increase in T_m was proportional to ligand concentration, as expected from eq 8.

Converting changes in T_m to an accurate binding constant requires knowledge of the unfolding enthalpy ($\Delta_U H$). Figure 3A shows the expected effect of ligand concentration on T_m for proteins with varying $\Delta_U H$. Proteins with lower $\Delta_U H$ will show a larger increase in T_m for a given concentration of ligand than proteins with larger $\Delta_U H$. Thus, an accurate assessment of $\Delta_U H$ was crucial to obtaining accurate ligand binding affinities. For a given protein, however, $\Delta_U H$ is the same regardless of the ligand being tested.

Given a protein that exhibits equilibrium two-state unfolding behavior, the $\Delta_U H$ obtained from the curves in Figure 2 is the van't Hoff enthalpy of unfolding (eq 6). Unfortunately, many proteins unfold in an irreversible manner, making the accuracy of this method for obtaining $\Delta_U H$ unreliable. This is seen intuitively in Figure 2B, where unfolding at increasing concentrations of TFSMA is expected to give curves that are sharper, because the unfolding enthalpy increases with T_m. In practice, however, the shape of the unfolding transition could become sharper, broader, or remain unchanged: sharper if unfolding is rapid and reversible and broader if unfolding is kinetically limited and inhibitors slow the unfolding rate. Regardless, at a constant heating rate, equilibrium binding ligands will raise the apparent T_m of proteins and fitting data to eq 6 gave an accurate midpoint, or T_m.

Figure 3B shows simulated curves of T_m as a function of total ligand concentration for ligands with varying K_b. Tighter binding ligands are expected to raise T_m to a higher extent when all other variables remain the same (eq 8). For a given protein, however, all ligands (at concentrations greater than the K_d) give a similar change in T_m vs ligand concentration; i.e., the terminal slopes in Figure 3B are identical, since they are determined by $\Delta_U H$. In practice, a calorimetrically determined $\Delta_U H$ was used to obtain K_d from T_m measured at several inhibitor concentrations. The curves in Figure 3B do not saturate; at higher ligand concentrations a larger shift in protein melting temperature is expected (eq 8).

Differential Scanning Calorimetry (DSC) of Carbonic Anhydrase. Thermodynamics of carbonic anhydrase II unfolding were studied by DSC using various solution conditions previously demonstrated to give varying T_m using ThermoFluor. Figure 4A shows representative thermograms in several buffers of varying pH, inhibitor, and dye concentration. Addition of ANS (50 μM) and DMSO (2.5%) decreased the T_m slightly, but by a statistically significant amount. This observation was consistent with ThermoFluor experiments, where the affinity of ANS for non-native CAII was estimated to be ~100 μM by measuring the change in intensity on unfolding vs ANS concentration. This small destabilization by ANS interacting with non-native species is expected to be independent of inhibitor interactions with native protein. Protein stability could be altered dramatically by changing pH or by adding a known inhibitor. For example, lowering the pH to 5.3, 4.8, or 4.4 lowered the T_m by 8, 16, or 25 °C, respectively. Alternatively, addition of 100 μM ACTAZ increased the T_m by ~8 °C. Figure 4B shows CAII melting temperature as a function of pH in PIPES and acetate buffers. Thermal stability was essentially pH independent between pH 5.8 and 8.0. Below pH 6, the T_m gradually decreased as the pH became more acidic, as expected for a protein that binds protons more tightly in the non-native state.

The calorimetric enthalpy of unfolding ($\Delta_U H_{cal}$) was calculated as the area of the unfolding peak, normalized to the molar protein concentration. The unfolding enthalpy was linearly proportional to T_m, and the slope of $\Delta_U H_{cal}$ vs T_m yielded $\Delta_U C_p = 4000$ cal mol^{-1} K^{-1} (Figure 4C), a value similar to that seen for the change in baseline on unfolding in Figure 4A. Experimental DSC curves were also fit to an equilibrium two-state unfolding model to obtain van't Hoff enthalpies, resulting in values nearly equal to those obtained using calorimetric enthalpies (Figure 4C). The $\Delta_U C_p$ value determined using van't Hoff enthalpy was similar: 3600 cal mol^{-1} K^{-1}. A summary of carbonic anhydrase thermodynamic stability obtained using DSC and ThermoFluor is given in Table 1, as are stability parameters extrapolated to 60 °C, as is the convention.

Concentration Response Curves (CRC) To Determine Binding Affinity and Stoichiometry from Changes in Thermal Stability. Figure 5A shows the T_m of human carbonic anhydrase I as a function of ligand concentration for four of the six inhibitors studied. For each ligand, T_m was measured in quadruplicate (standard deviation <0.2 °C) and was

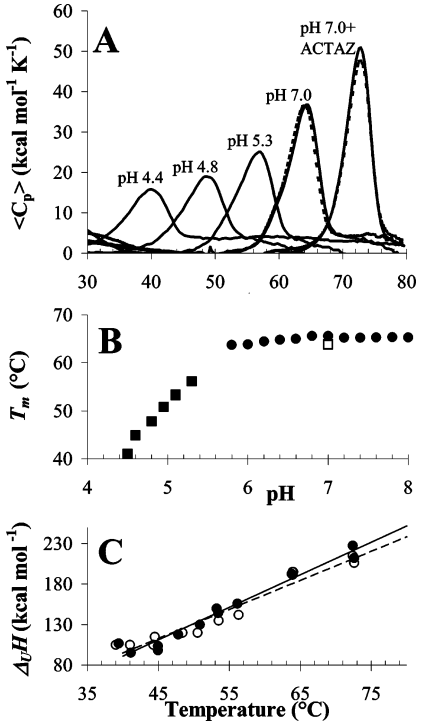

FIGURE 4: Differential scanning calorimetry of *b*-CAII gave $\Delta_U H$ and $\Delta_U C_p$. (A) Excess enthalpy is shown as a function of temperature for *b*-CAII (0 or 5 μM) in buffer (50 mM sodium acetate pH 4.4, 4.8, or 5.3, or in 25 mM PIPES, 100 mM NaCl, 0.5 mM EDTA at pH 7.0). Additions to buffer included 50 μM ANS (dotted line at pH 7.0) and/or 100 μM ACTAZ (solid, dotted line with peaks at 75 °C). DSC scans were collected at 1 °C/min; the pH for each experiment is indicated in the figure. The area under the curve gave the calorimetric unfolding enthalpy. Conditions giving lower T_m also gave smaller areas due to the positive heat capacity of unfolding. As expected, ACTAZ raised the melting temperature, whereas ANS gave a small but statistically significant decrease in T_m. (B) Thermal stability was measured in buffers of varying pH (Figure 4A), using acetate (■) or PIPES plus 0 (●) or 50 μM ANS (□). (C) Calorimetric unfolding enthalpy calculated from area of data in Figure 4A (●, solid line) was determined at multiple pH values, where the T_m varied by over 20 °C (Figure 4B). Enthalpy vs T_m was fit to a linear function; the slope defined $\Delta_U C_p = 4.0$ kcal mol^{-1} K^{-1}. A consistent effect is seen in Figure 4A, where the baseline after unfolding shifts upward by 4−5 kcal mol^{-1} K^{-1}. van't Hoff enthalpies of protein unfolding obtained by fitting DSC curves to a two-state model (○, dotted line) gave a nearly identical heat capacity: ~3.6 kcal mol^{-1} K^{-1}.

Table 1: Thermodynamics of Carbonic Anhydrase I and II Stability

parameter	*h*-CA I[a,b]	*b*-CA II[a,b]
T_m (°C)	59 ± 0.2	64 ± 0.2
$\Delta_U H_{T_m}$ (kcal mol^{-1})[c]	nd	190 ± 20
$\Delta_U S_{T_m}$ (kcal mol^{-1} K^{-1})[c]	nd	0.56
$\Delta_U C_p$ (kcal mol^{-1} K^{-1})[c,d]	nd	3.8 ± 0.4
ThermoFluor		
$\Delta_U H_{T_r}$ (kcal mol^{-1})[e]	140 ± 20	170 ± 20
Reference		
$\Delta_U G_{T=60°C}$ (kcal mol^{-1})[f]	−430	+2.2
$\Delta_U H_{T=60°C}$ (kcal mol^{-1})[f]	144	174
$\Delta_U S_{T=60°C}$ (kcal mol^{-1} K^{-1})[f]	0.43	0.52

[a] Standard deviation or uncertainty (whichever is greater) is shown. [b] Parameters for CAII were determined by DSC (Figure 4) and ThermoFluor, for CAI by ThermoFluor only. [c] Calorimetric parameters for protein unfolding at T_m, obtained by DSC. [d] Heat capacity of protein unfolding obtained from $\Delta\Delta_U H_{T_m}$ vs ΔT_m (Figure 4C). [e] Protein unfolding enthalpy obtained from ThermoFluor (Figure 2, fit using eq 6). [f] Thermodynamic parameters extrapolated to reference temperature of 60 °C using eq 4.

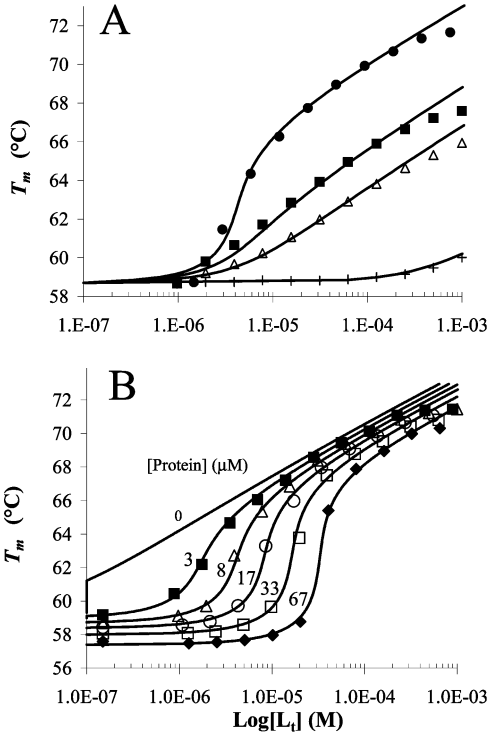

FIGURE 5: Concentration effect of ligand and protein on T_m. (A) The effect of increasing ligand concentration on T_m. Reactions contained 4 μL of 8.3 μM *h*-CA I in 25 mM MES pH 6.1, 50 mM NaCl, 2% DMSO, and 50 μM ANS plus indicated concentrations of TFMSA (●), METHZ (■), ACTAZ (△), and SULFA (+). Symbols represent average T_m obtained from quadruplicate ThermoFluor melts. The largest standard error of the quadruplicates (0.2 °C) is smaller than the symbol size. Solid lines are simulated according to eq 14, using $\Delta_U H = 120$ kcal mol^{-1}, $\Delta_U C_p = 3.8$ kcal mol^{-1} K^{-1}, $T_m = 58.7$ °C, and K_{b,T_0} values of 1.2×10^8, 3.2×10^6, 1.3×10^6, and 4.0×10^3 M^{-1}, respectively. (B) Sigmoidicity in T_m vs ligand concentration gives binding stoichiometry. *h*-CAI thermal stability was monitored in quadruplicate by ThermoFluor as a function of TFMSA; concentration of protein: 0 μM (no symbols, theoretical limit), 3.3 μM (■), 8.3 μM (△), 17 μM (○), 33 μM (□), or 67 μM (◆). T_m in the absence of ligand is dependent on protein concentration and was 59.3, 59.0, 58.7, 58.4, 58.0, and 57.4 °C, respectively.

concentration dependent. Data in Figure 5A were used to calculate the binding affinity at T_m using eq 14 and the calorimetrically measured parameters for protein stability (Table 1). Simulated curves represented the experimental data well and yielded K_{d,T_m}. Binding constants at T_m were extrapolated to 37 °C using eq 10, assuming "average" ligand binding thermodynamics: $\Delta_b H = -5$ kcal mol^{-1} and $\Delta_b C_p = -200$ cal mol^{-1} K^{-1}.

Figure 5B shows sigmoidal concentration response curves for the T_m of *h*-CAI as a function of TFMSA, using five concentrations of protein. In the absence of ligand, the protein melting temperature decreased slightly with increasing protein concentration, because *h*-CAI unfolding was irreversible and aggregation is a higher order reaction. In the presence of ligand, the concentration response curves in Figure 5B showed three distinct regions corresponding to substoichiometric amounts of ligand, concentrations of protein and ligand that were approximately equal, and saturating concentrations of ligand. At substoichiometric ligand concentrations, little detectable change in the T_m was

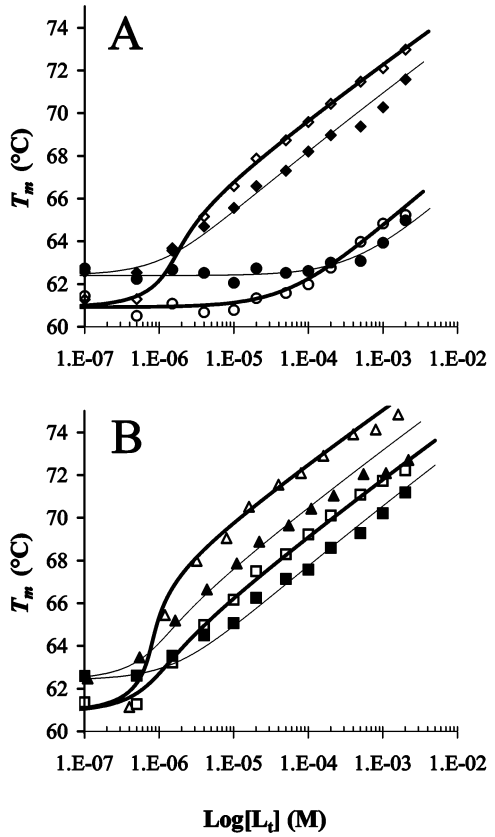

FIGURE 6: Zinc effect on inhibitor binding to b-CAII. Concentration response curves of inhibitor binding to *b*-CAII in 25 mM PIPES, pH 7.0, 100 mM NaCl, 0.5 mM EDTA (open symbols) or 25 mM PIPES, pH 7.0, 100 mM NaCl, 50 μM $ZnCl_2$ (closed symbols) were obtained by ThermoFluor in quadruplicate (as in Figure 5) and fit to eq 14 to give values in Table 2. Inhibitors used include (A) DCHPA (triangles), METHZ (squares) and (B) ACTAZ (diamonds), PAMBS (circles).

observed. When the ligand concentration was approximately equal to protein (0.2[protein] < [ligand] < 5[protein]), a sharp sigmoidal increase in melting temperature was observed. When ligand concentration was much greater than protein concentration, the T_m increased further. By examining the relationship of ligand and protein concentrations and observed changes in T_m, one can assess the stoichiometry of the interaction, assuming reasonable confidence in the concentration of active ligand and protein. For TFMSA and either *h*-CAI or *b*-CAII, the dependence of T_m on ligand and protein concentration is consistent with a 1:1 stoichiometry. When the same experiment was run using more weakly binding ligands (e.g. METHZ, ACTAZ, SULFA in Figure 5A), a set of concentration response curves was obtained that showed no sigmoidicity, making determination of stoichiometry indeterminable at this protein concentration.

Effect of Zinc on Inhibitor Binding. Carbonic anhydrase contains a single zinc ion at the active site, necessary for activity. To test whether adding Zn^{2+} affected inhibitor binding, ThermoFluor experiments were carried out in the presence of 50 μM $ZnCl_2$ (sufficient to fill any unoccupied sites) or in the presence of 0.5 mM EDTA (sufficient to chelate free zinc yet not remove the active site metal). Figure 6 shows concentration response curves of ACTAZ and PAMBS in the presence of Zn^{2+} or EDTA at pH 7. Zn^{2+} affected both the protein stability and the observed ligand binding affinity. In the absence of inhibitor, Zn^{2+} itself acted as ligand, increasing the T_m. At higher concentrations, Zn^{2+} destabilized the protein, perhaps by increasing aggregation of non-native species (data not shown). In the presence of Zn^{2+}, inhibitors showed a smaller increase in T_m at a given concentration; i.e., binding to CA was ~10-fold weaker in the presence of zinc (Figure 6, Table 2). Crystallographic data confirm that the sulfonamide group of these inhibitors interacts with the zinc ion bound at the active site (*18*). However, if sulfonamides have weak affinity for Zn^{2+} in the unbound state, a decrease in observed affinity would be expected, since the concentration of available inhibitor would be reduced.

Table 2: ThermoFluor Derived Sulfonamide Inhibitor Binding Constants[d]

	h-CA I			*b*-CA II		
inhibitor	pH 6[a]	pH 7, $ZnCl_2$[b]	pH 7, EDTA[c]	pH 6[a]	pH 7, $ZnCl_2$[b]	pH 7, EDTA[c]
ACTAZ	2.4×10^5	1.1×10^6	8.0×10^5	1.0×10^6	4.5×10^6	5.0×10^7
METHZ	5.0×10^5	2.5×10^7	8.0×10^6	7.0×10^5	3.5×10^6	3.5×10^7
TFMSA	1.0×10^8	3.0×10^7	1.0×10^8	3.0×10^6	5.0×10^6	8.0×10^7
DCHPA	2.0×10^4	3.2×10^6	5.0×10^5	4.0×10^6	2.8×10^7	3.5×10^8
SULFA	8.0×10^2	3.5×10^3	8.0×10^3	2.5×10^3	1.4×10^4	1.0×10^5
PAMBS	Too weak	4.0×10^3	1.0×10^4	3.0×10^2	7.0×10^3	7.0×10^4

[a] Conditions: 25 mM MES, pH 6.1, 100 mM NaCl. [b] Conditions: 25 mM PIPES, pH 7.0, 100 mM NaCl, 50 μM $ZnCl_2$. [c] Conditions: 25 mM PIPES, pH 7.0, 100 mM NaCl, 0.5 mM EDTA. [d] K_{b,T_0} obtained from ThermoFluor concentration dependent effects on T_m. Observed binding constants were extrapolated to 37 °C using $\Delta_b H_{T_0} = -5.0$ kcal mol^{-1} and $\Delta_b C_p = -300$ cal mol^{-1} K^{-1}.

Interestingly, the binding exhibited significant pH dependence, being uniformly ~50-fold tighter at pH 7 for *b*-CAII. Data with *h*-CAI were less uniform, varying from 20-fold weaker (DCHPA, METHZ) to no different at pH 6 (TFMSA). These effects are consistent with inhibitor binding being linked to a series of protonation events including the pK_a of unbound sulfonamide and the pK_a of CA zinc-bound hydroxide (*19*).

Correlation between Binding Constants Determined by ITC and ThermoFluor. Analysis of the ligand concentration effect on T_m gave an accurate determination of binding affinity *at the* T_m. As with any in vitro derived data, a comparison of values measured under varying conditions should include a correction for parameters that change in predictable manners. To compare binding affinity by ThermoFluor (i.e. at the T_m) with that measured by other means requires extrapolating binding affinities to physiological temperatures. Such extrapolations are straightforward (*20*) but benefit from an accurate knowledge of the enthalpy and heat capacity of ligand interaction (eq 10). In the absence of binding enthalpy information, an "average" $\Delta_b H$ and $\Delta_b C_p$ were used (Table 2).

An extensive analysis of binding enthalpies was done using isothermal titration calorimetry to deconvolute steps in the binding process that contribute to the temperature dependence of binding (*19*). This technique not only gave an independent determination of the binding affinity but also gave an experimental measure of $\Delta_b H_{obs}$ and $\Delta_b S_{obs}$. The heat capacity of binding ($\Delta_b C_p$) was obtained by analyzing calorimetric enthalpy at various temperatures. These measured binding enthalpies and heat capacities were then used to extrapolate

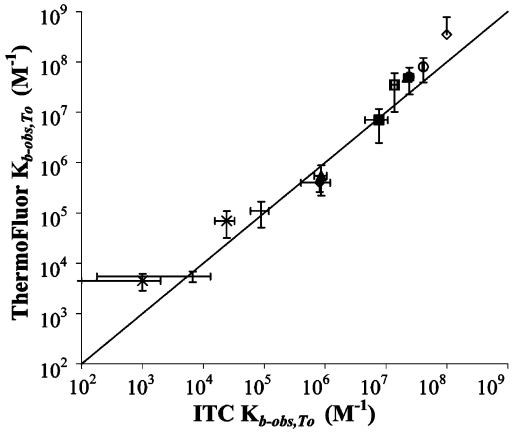

FIGURE 7: Correlation of binding constants obtained by ThermoFluor and ITC. ThermoFluor derived binding constants, extrapolated to 37 °C using approximate values for ligand binding enthalpy and heat capacity ($\Delta_b H_{T_0} = -5.0$ kcal mol^{-1}, $\Delta_b C_p = -300$ cal mol^{-1} K^{-1}) are compared to values obtained from ITC measurements. The solid line shows the trend of exact match between the two methods for *h*-CAI (filled symbols) or *b*-CAII (open symbols) at pH 7.0 using ACTAZ (triangles), METHZ (squares), TFMSA (circles), DCHPA (diamonds), SULFA (+) or PAMBS (*). The correlation is good within the error of each method. Note that all inhibitors bind more strongly to *b*-CAII than to *h*-CAI. An especially large difference was observed for DCHPA.

ThermoFluor binding constants at the T_m to 37 °C. For carbonic anhydrase, the difference between using assumed "average" thermodynamic binding parameters or calorimetrically measured binding parameters was small. Figure 7 shows a correlation between the binding constants determined by ITC and those measured by ThermoFluor extrapolated to 37 °C. Overall, an excellent correlation was seen between the two methods, for both forms of carbonic anhydrase, over the entire range of five orders of magnitude.

DISCUSSION

A classical method for estimating ligand binding affinities is by measuring the effect of a ligand on stability using chemical or thermal denaturation methods (*21*). These methods are attractive due to their general nature, the wide variety of applicable systems that can be studied, and the rigorous theoretical interpretation that has been developed. Data interpretation may follow either equilibrium or kinetic arguments, since equilibrium binding ligands should slow both the *rate* of denaturation and shift the equilibrium between native and non-native forms. An assumption is often adopted to simplify data interpretation: either unfolding is irreversible (and thus kinetically limited) or unfolding is fully reversible and the system is at equilibrium at all times. In an experiment where stability is monitored as the temperature is steadily increased, either kinetic or equilibrium theory would dictate equilibrium binding ligands cause the midpoint of an unfolding transition to occur at a higher temperature.

Reversibility of folding is often difficult to demonstrate, being highly dependent on the stability of non-native species and their tendency to self-associate and form aggregates. Reversibility is enhanced when conditions are chosen to minimize interaction of hydrophobic surfaces prone to cause aggregation, either by reducing concentration or by choosing buffer composition wisely. Because aggregation is a higher ordered reaction, reversibility is enhanced at low concentration. Likewise, including excipients that may interact with exposed hydrophobic surfaces is likely to reduce aggregation. Interestingly, Kundu and Guptasarma (*16*) showed that a hydrophobic dye (ANS) could prevent heat-induced aggregation of carbonic anhydrase, thus enabling reversible thermal denaturation for this protein. Analysis of ligand concentration effect on protein thermal denaturation presented here assumes equilibrium, reversible, unfolding conditions.

High-throughput thermal denaturation measurements significantly increased the ability to study the effects of ligands on protein stability. Due to the parallel nature of the assay and the low protein requirements (50−500 ng/well), ThermoFluor enabled analysis of numerous replicates over wide concentration ranges with multiple inhibitors under varying conditions. Precise determinations of T_m with varying ligand concentration led to a thorough experimental confirmation of models describing ligand stabilization of protein. Previous equilibrium-unfolding models that calculate binding affinity from changes in protein T_m have been expanded to include consideration of free ligand depletion by that bound to protein. These new models agree well with the experimental data and suggest that, for a given protein with a defined $\Delta_U H$, all ligands are expected to have similar concentration dependence at concentrations above their K_d. This was experimentally observed for all of the inhibitors studied.

Calculations including the reduction in free ligand and protein by that which is bound in the complex demonstrate an additional benefit of using stability perturbations to measure affinity: the ability to obtain binding stoichiometry. Two inhibitors bound with sufficient affinity that plots of T_m vs ligand concentration were sigmoidal due to depletion of total ligand by that which was bound. In a pharmaceutical environment, compounds in combinatorial chemical libraries may be at unknown concentrations, due to degradation, solubility, stability, and/or the presence of chiral centers.

In general, the shapes of the concentration response curve (Figures 3, 5 and 6) are revealing in assessing the details of inhibitor binding. Whereas equilibrium-binding ligands give the expected concentration dependence of T_m, other ligands show a saturating effect on protein T_m. This can occur for several reasons: (1) the ligand solubility is limited, (2) the ligand has appreciable affinity for both native and non-native forms of the protein, or (3) the ligand is a covalent modifier. Saturation in ΔT_m at ligand concentrations in excess of the protein most often occur because the ligand reaches a solubility limit (e.g. concentrations at 0.5 mM and above in Figure 5), which can also be detected by light-scattering techniques. Alternatively, ligands that have appreciable affinity for both native and non-native forms of a protein may only shift the equilibrium to a limited extent; at concentrations above the weaker of the two affinities, no further shift in equilibrium will be observed. Finally, the effect of an irreversible covalent ligand on the protein T_m is saturated after reaching a concentration equal to the reaction stoichiometry. In yet other cases, some inhibitors found by screening combinatorial libraries *destabilize* proteins (*22*). Such compounds typically lack specificity, destabilizing many proteins. Thus, when ranking lead molecules through stability perturbations, valuable mechanistic information is obtained by examining the concentration response of ligand on T_m.

One limitation to ranking ligand binding by measuring perturbations in thermal stability is that the binding constant obtained is most accurate at T_m and must be extrapolated to physiological temperature, either to assess efficacy or to compare assays. It should be noted that this same concern applies to any assay run at nonphysiological temperatures. The extrapolation of binding constants is more accurate if the van't Hoff enthalpy of binding is known. Temperature extrapolation of K_d in the absence of binding thermodynamics gives the same rank ordering as obtained at the T_m. For sulfonamide inhibitors of carbonic anhydrase, a similar rank ordering was obtained using calorimetrically determined binding enthalpy and heat capacity to extrapolate K_{d,T_m} to 37 °C, because all inhibitors bound with similar thermodynamic parameters.

Direct binding assays have numerous advantages when ranking lead compounds for structure−activity relationship purposes. First, binding assays have general applicability to many different target proteins. Second, complimentary binding assays can be obtained in the presence or absence of known ligands and/or substrates to identify binding sites through competition or to examine binding cooperativity, allowing separation of the structure−activity relationship of ligand binding from that of ligand activity. The IC_{50} values yielded by many assays do not distinguish the mechanism or site of compound action; thus, several dissimilar series of compounds may show the same activity due to interactions at different sites. Third, binding assays can reveal mechanistic information such as stoichiometry or distinguishing covalent vs noncovalent interactions. Thus, a general high-throughput binding assay should be seen as a tool complimentary (but orthogonal) to classical methods of determining ligand activity, one that may simplify structure−activity relationship analysis.

REFERENCES

1. Murphy, K. P. (2001) Protein Structure, Stability, and Folding, *Methods Mol. Biol. 168*.
2. Brandts, J. F., and Lin, L. N. (1990) Study of strong to ultratight protein interactions using differential scanning calorimetry, *Biochemistry 29*(29), 6927−6940.
3. Freire, E. (1995) Differential scanning calorimetry, *Methods Mol. Biol. 40*, 191−218.
4. Sturtevant, J. (1987) Biochemical applications of differential scanning calorimetry, *Annu. Rev. Phys. Chem. 38*, 463−488.
5. Xie, D., Fox, R., and Freire, E. (1994) Thermodynamic characterization of an equilibrium folding intermediate of staphylococcal nuclease. *Protein Sci. 3*(12), 2175−2184.
6. Meeker, A. K., Garcia-Moreno, B., and Shortle, D. (1996) Contributions of the ionizable amino acids to the stability of staphylococcal nuclease, *Biochemistry 35*(20), 6443−6449.
7. Royer, C. A. (1995) Fluorescence spectroscopy, *Methods Mol. Biol. 40*, 65−89.
8. Weber, P. C., et al. (1989) Structural origins of high-affinity biotin binding to streptavidin, *Science 243*(4887), 85−88.
9. Pantoliano, M. W., et al., (2001) High-density miniaturized thermal shift assays as a general strategy for drug discovery, *J. Biomol. Screen 6*(6), 429−440.
10. Sly, W. S., and Hu, P. Y. (1995) Human carbonic anhydrases and carbonic anhydrase deficiencies. *Annu. Rev. Biochem. 64*, 375−401.
11. Lindskog, S. (1997) Structure and mechanism of carbonic anhydrase, *Pharmacol. Ther. 74*(1), 1−20.
12. Thoms, S. (2002) Hydrogen bonds and the catalytic mechanism of human carbonic anhydrase II, *J. Theor. Biol. 215*(4), 399−404.
13. Shrake, A., and Ross, P. D. (1992) Origins and consequences of ligand-induced multiphasic thermal protein denaturation, *Biopolymers 32*(8), 925−940.
14. Robertson, A. D., and Murphy, K. P. (1997) Protein Structure and the Energetics of Protein Stability. *Chem. Rev. 97*(5), 1251−1268.
15. Gomez, J., et al. (1995) The heat capacity of proteins, *Proteins 22*(4), 404−412.
16. Kundu, B., and Guptasarma, P. (1999) Hydrophobic dye inhibits aggregation of molten carbonic anhydrase during thermal unfolding and refolding, *Proteins 37*(3), 321−324.
17. Slavik, J., et al. (1982) Anilinonaphthalene sulfonate fluorescence and amino acid transport in yeast, *J. Membr. Biol. 64*(3), 175−179.
18. Stams, T., and Christianson, D. W. (2002) X-ray crystallographic studies of mammalian carbonic anhydrase isozymes, *EXS* (90), 159−174.
19. Matulis, D. and Todd, M. (2004) Thermodynamics/Structure Correlations of Sulfonamide Inhibitor Binding to Carbonic Anhydrase in *Biocalorimetry 2* (Ladbury, J. and Doyle, M., Eds.) Wiley & Sons, New York.
20. Waldron, T. T., and Murphy, K. P. (2003) Stabilization of proteins by ligand binding: application to drug screening and determination of unfolding energetics, *Biochemistry 42*(17), 5058−5064.
21. Murphy, K. P., Ed. (2001) Protein Structure, Stability, and Folding, *Methods Mol. Biol. 168*.
22. Todd, M. J., and Salemme, F. R. (2003) Direct Binding Assays for Pharma Screening. *Genetic Eng. News 23*(3).

BI048135V